American Mineralogist, Volume 83, pages 925–930, 1998

Direct identification of the six polytypes of chlorite characterized by semi-random stacking

TOSHIHIRO KOGURE* AND JILLIAN F. BANFIELD

Mineralogical Institute, Graduate School of Science, University of Tokyo, Hongo, Tokyo 113-0033, Japan

ABSTRACT

This paper demonstrates that the six standard polytypes of chlorite, whose definitions are based on the orientation of the interlayer sheet and the position of the interlayer sheet on the 2:1 layer, can be discriminated by atomic-resolution images recorded down [010], using a transmission electron microscope with a ~2 Å point resolution and digital image processing. Several specimens were investigated to reveal their local stacking structures. A I*bb* chlorite is highly twinned and twin boundaries consist of a II*b*+I*a* stacking sequence at the interlayer sheet. An interstratified chlorite/biotite formed by hydrothermal alteration from biotite in granite consists of a mixture of several chlorite polytypic sequences, including I*ab*, I*bb*, II*ab*, and II*bb*. These polytypic details of chlorite and other sheet silicates provide important insights into mineral stability, origin, and reaction mechanisms.

INTRODUCTION

Chlorite is a common and important layer silicate formed under a wide range of conditions. Its crystal structure consists of a T-O-T (tetrahedral-octahedral-tetrahedral) or 2:1 layer and a brucite-like interlayer (Fig. 1). Brown and Bailey (1962) theoretically derived 12 different 1-layer polytypes that arise due to the structural relation between the T-O-T layer and brucite-like interlayer. They also showed that these 12 polytypes can be classified into six ideal groups if they have semi-random stacking (the position of the repeating 2:1 layer on the interlayer adopts a random mixture of three equivalent positions related to each other by *b*/3 shifts). Because most natural chlorites contain semi-random stacking, assignment to one of these six groups (I*aa*, I*bb*, II*aa*, II*bb*, I*ba*, and II*ab*; Bailey 1988a) is common. I and II indicate whether the slant direction of the octahedra in the brucite-like interlayer and that in the T-O-T layer is the same (I) or opposed (II), and "*a*" and "*b*" indicate the way in which interlayer sites project onto the cation and hydroxyl sites in the T-O-T layers above and below (Fig. 2; Bailey 1988b). The most common polytype in nature is II*bb*. Its abundance is attributed to the *b*-type interactions minimizing repulsion between the tetrahedral and inter-

* E-mail: kogure@min.s.u-tokyo.ac.jp

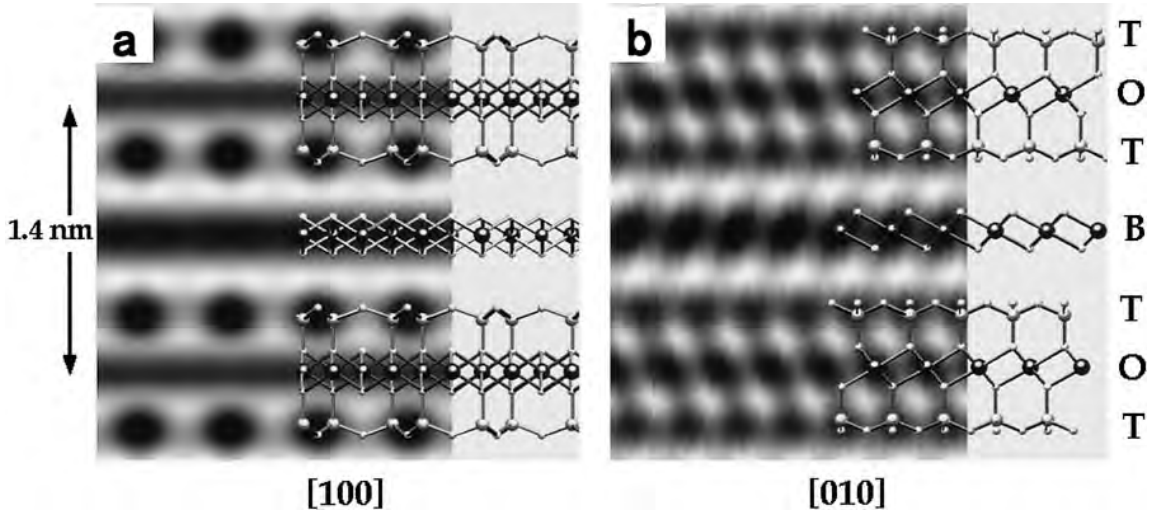

FIGURE 1. The crystal structure of chlorite (II*bb*) and corresponding simulated images down (**a**) [100] and (**b**) [010]. Simulation parameters are: defocus = −40 nm (Scherzer focus); specimen thickness = 2 nm; and the composition assumed at all octahedral sites is $Mg_{0.5}Fe_{0.5}$.

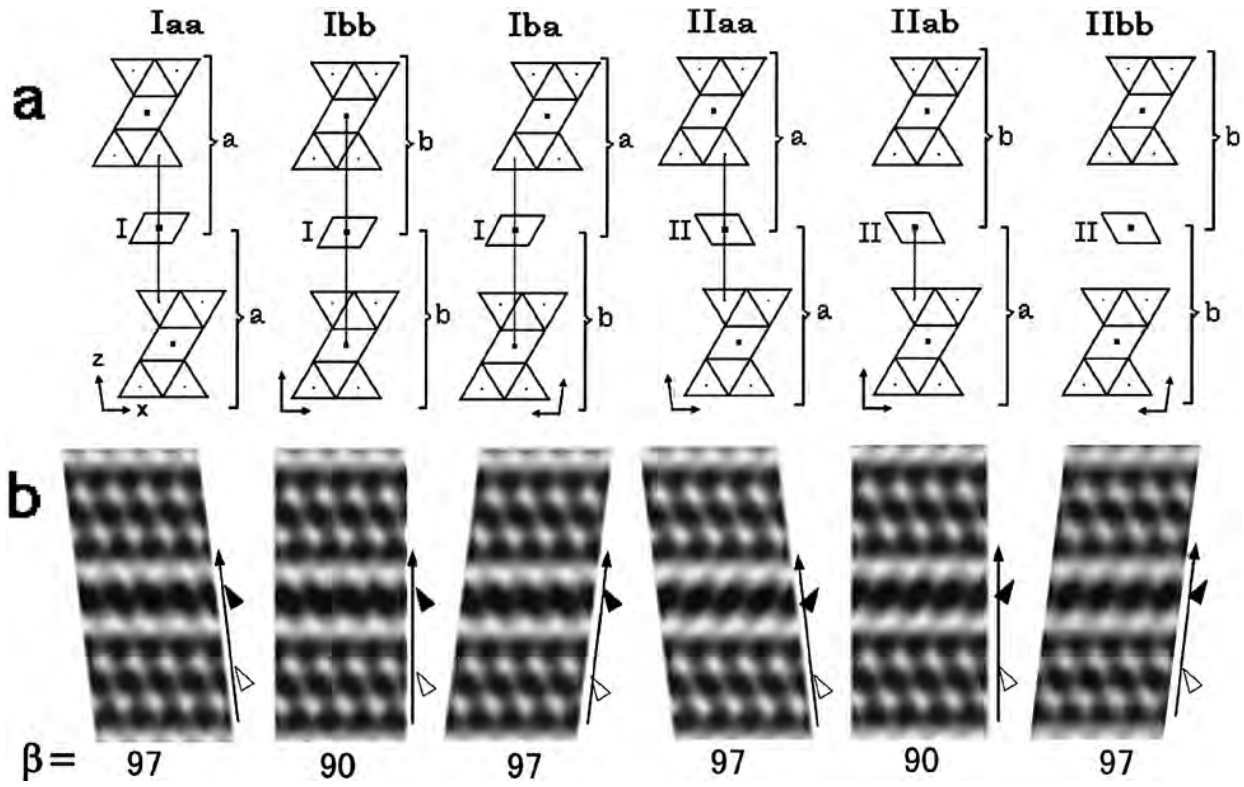

Figure 2. (**a**) [010] diagrammatic views of the six chlorite polytypes (modified from Bailey 1988b) and (**b**) corresponding simulated images. The parameters for the simulations are the same as those in Figure 1. In b, the long arrows, black arrow-heads, and white arrow-heads, respectively, indicate the *c* axis, the slant of octahedra in the interlayer, and the slant in the T-O-T layer.

layer cations and the type II arrangement optimizing interactions between cations in the two octahedral sheets. Two polytypes (II*aa* and II*ab*) have yet to be found (Bailey 1988b). The stabilities of these polytypes as a function of chemical composition (Brown and Bailey 1962) or with temperature and/or pressure (Walker 1993; Jullien et al. 1996) have been discussed.

Brown and Bailey (1962) and Bailey (1988a) showed that X-ray diffraction (XRD) patterns can be used to distinguish the six polytypes and Banfield and Bailey (1996) reported that intensity variations in selected area electron diffraction patterns can serve a similar role. However, electron diffraction methods require relatively homogeneous areas of at least several tens of nanometers (tens of micrometers in the case of X-ray). Thus, these techniques have limited utility for studies that require few or even single unit cell-scale resolution to distinguish reaction mechanisms and to explain the origin of specific polytypes. For example, chlorite forms interstratified structures with other sheet silicates (mica, serpentine, etc.) but generally their polytypes have not been determined, even though this information can place important constraints on the reaction mechanism (e.g., Banfield and Murakami 1998). High-resolution transmission electron microscopy (HRTEM) is the logical approach to polytype determination. In most previous studies of chlorite (e.g., Bons and Schryvers 1989; Banfield and Bailey 1996; Kogure and Murakami 1998), HRTEM observations were recorded down [100] (or the equivalent [110] or [1$\bar{1}$0] directions in semi-randomly stacked chlorite; see Fig. 1a). However it is impossible to discriminate all six systems from such images. Recently it was demonstrated that [010] images provide important polytypic information necessary for understanding the vermiculitization of chlorite (a II*bb* or I*bb* to I*aa* transformation; Banfield and Murakami 1998). The current paper shows that all six polytypes can be discriminated from one HRTEM photograph recorded down [010].

Experimental methods

Multi-slice simulations were performed using MacTempas software (Kilaas 1991) using cell parameters and atomic coordinates from Brown and Bailey (1962). Polytype images down [010] were simulated for the JEOL JEM-2010 transmission electron microscope (TEM) used to record experimental images (200 kV, C_s = 0.5 mm, spread of focus = 10 nm, beam convergence semi-angle = 1.0 mrad, and spatial frequencies corresponding to an objective aperture = 5.0 nm^{-1}). Experimental images recorded on film were digitized using a CCD camera (Kodak Megaplus model 1.4i) and processed by rotational filtering (Kilaas 1998) implemented within Digital-Micrograph version 2.5 (Gatan Ltd.) to enhance the contrast from the crystal, as described below.

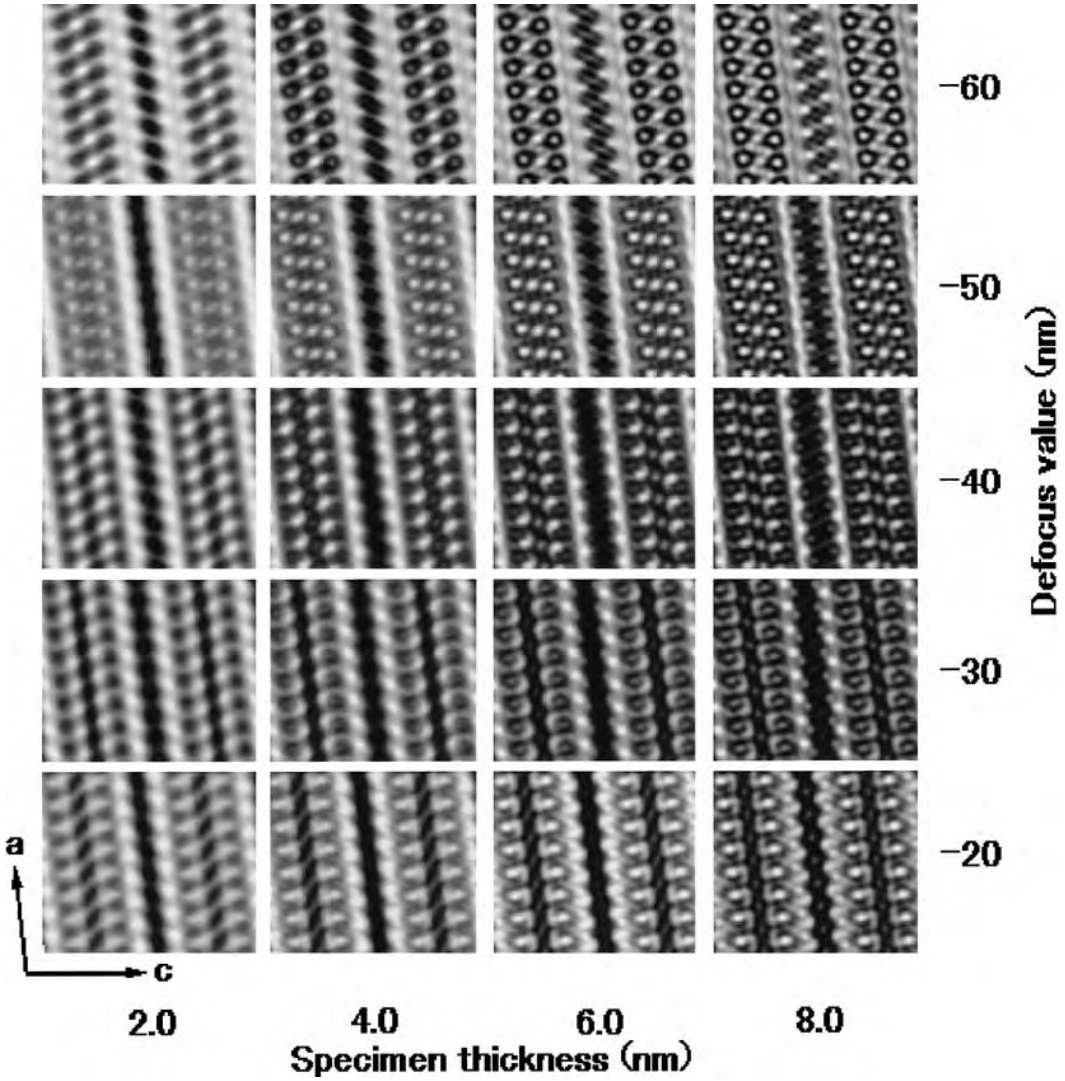

FIGURE 3. Simulated images for II*bb* chlorite down [010] as functions of defocus and specimen thickness. The assumed composition at all octahedral sites is $Mg_{0.5}Fe_{0.5}$.

Samples examined in this study were II*bb* chlorite from green schists, Nagatoro, Saitama-prefecture, Japan, and I*bb* chlorite from Tazawa mine, Akita-prefecture, Japan (Shirozu and Bailey 1965), and interstratified biotite/chlorite from Gogoshima, Ehime-prefecture, Japan (Kogure 1996). Specimens were prepared for TEM observation down [*hk*0] by argon ion milling (see Kogure and Murkami 1998 for details).

RESULTS AND DISCUSSION

Image simulations and data processing

The [100] zone axis images of II*bb*-2 tri-octahedral chlorite (equivalent to [110] and [1$\bar{1}$0] images in semi-randomly stacked chlorite) do not provide information about the slant of the octahedral sheet or the β angle (Fig. 1a). Instead, this information is carried by images recorded down [010] (equivalent to [310] and [3$\bar{1}$0] in semi-randomly stacked chlorites; Figs. 1b and 2). The β angle (90° or 97°) can be determined by inspection (Fig. 2). The dark spots in the interlayer have a slanted elliptical shape. Comparison with the simulation (Fig. 1b) shows that this spot shape is due to the projected potential of hydroxyls coordinating metal atoms. Consequently, the slant directions of octahedral sheets can be determined from the direction of slant of the ellipses. The slant of octahedra in the T-O-T layer is evident from the contrast due to the tetrahedral and octahedral cations (Fig. 1b). This result allows differentiation of type I from type II chlorite. Furthermore, for structures with β = 97°, the combination of the relationships between the *c* axis orientation and slants of two kinds of octahedra distinguishes I*aa*, II*aa*, I*ba*, and II*bb* (Fig. 2). We can also use the positional relation between ellipses in the interlayer and spots in adjacent tetrahedral sheets to identify ''*a*'' or ''*b*'' stacking.

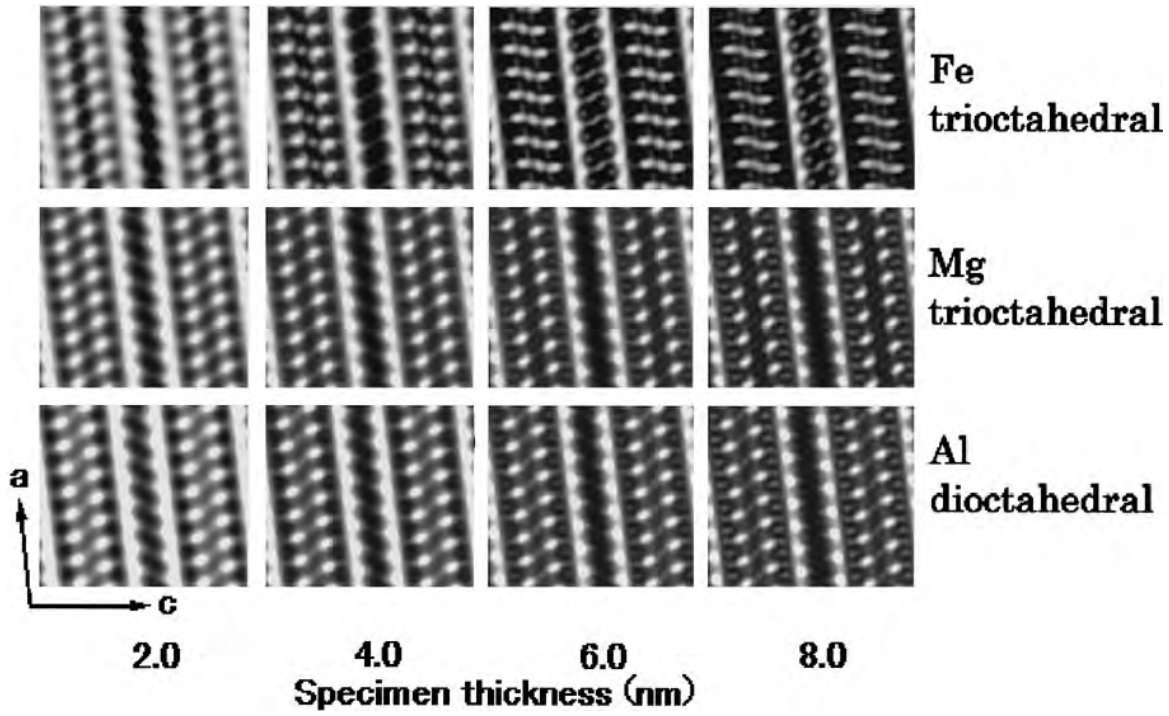

Figure 4. Simulated images for II*bb* chlorite down [010] as functions of the composition at octahedral sites and specimen thickness. The defocus value is −40 nm (Scherzer focus).

With increased sample thickness, the interlayer in II*bb* chlorite rapidly loses the diagnostic elliptical shape contrast (Fig. 3) whereas the correspondence between contrast and atomic positions in the T-O-T layer is preserved to greater specimen thickness (Fig. 4). This tendency is more distinct as the projected potential at octahedral sites increases. When all octahedral sites are fully occupied by Fe, the limit of thickness to identify the elliptical shape is only about 2 nm whereas it is about 7 nm in the case of Mg or dioctahedral Al chlorite (Fig. 4). As the detailed contrast at the interlayer is needed to discriminate the six polytypes, selection of the thinnest areas is critical. How-

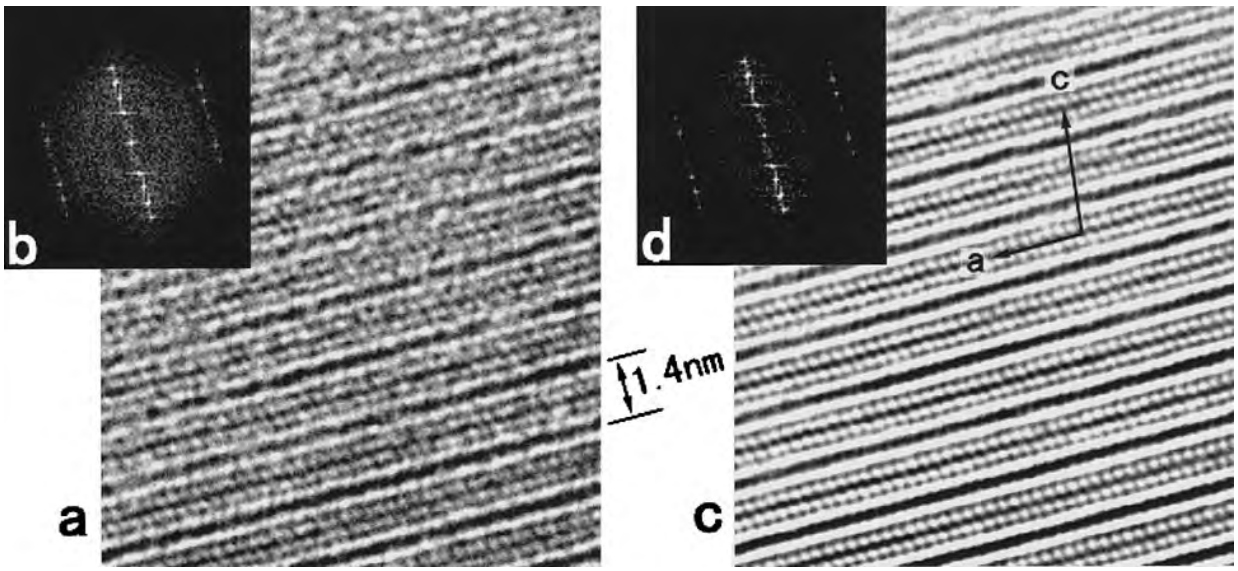

Figure 5. Observed HRTEM image down [010] of II*bb* chlorite in a green schist before (**a**) and after (**c**) rotational filtering. (**b**) and (**d**), Fourier transforms of the upper half of the images. The Mg/Fe ratio is about 1/2.

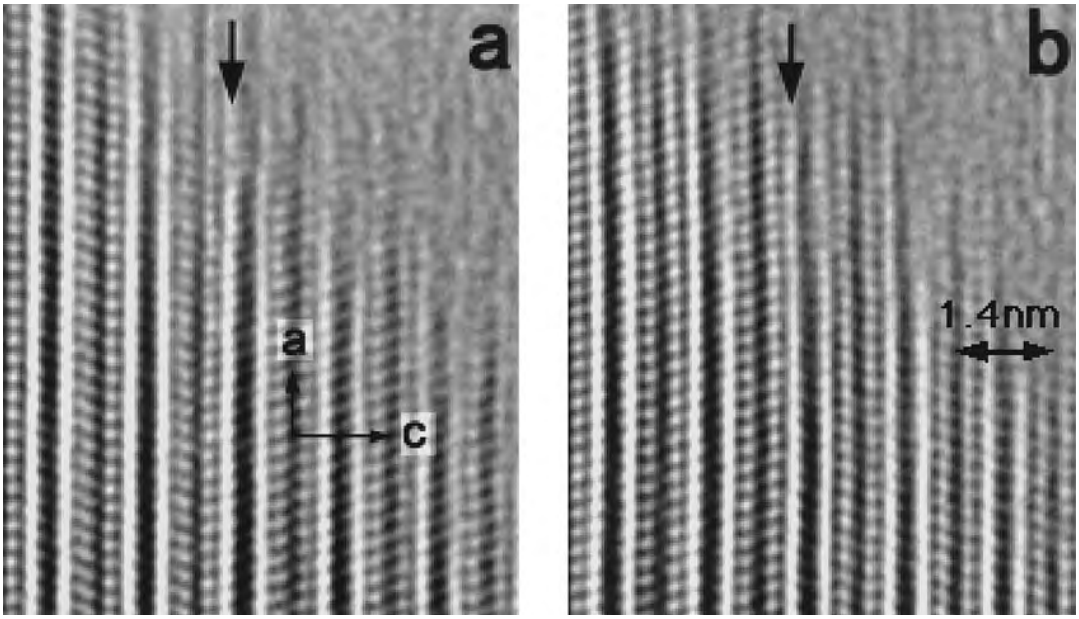

FIGURE 6. Filtered images of twinned I*bb* chlorite from Tazawa mine showing two adjacent twin boundaries (**a**) in the left and (**b**) in the right. The arrows indicate the twin plane where II*b* stacking sequence forms.

ever, in practice, the contrast of such thin crystals is weak and diminished by the superimposed contrast of amorphous materials formed by ion-milling, carbon coating, or beam damage. In the thin area of II*bb* chlorite (top of Fig. 5a), the contrast of the crystal is reduced by that of amorphous materials, resulting in a round cloud (Fig. 5b) in the Fourier transform (FT). The rotational filter is effective in removing the contrast of amorphous material and making periodic contrast distinct (Kilaas 1998). The brucite-like interlayer structure is apparent in the processed image and its FT from the thin area (Figs. 5c and 5d) and we can observe that all layers have the II*bb* sequence.

Examples of determination of local chlorite structures

Ibb chlorite from Tazawa mine. This specimen is similar to that used to refine the crystal structure of I*bb* chlorite by XRD (Shirozu and Bailey 1965). They noted that reflections with $k \neq 3n$ are streaked parallel to the c^* axis, indicating semi-random stacking, and reported (001) twinning, based on the intensity distribution in XRD (this twinning does not generate extra spots because $\beta = 90°$). These features are confirmed here. Bright field images of the specimen with the incident beam slightly tilted from [010] show that the crystal is divided into packets a few tens of nanometers thick bounded by (001). HRTEM images of the boundaries in the left (Fig. 6a) and right (Fig. 6b) of a packet indicate that this polytype is definitely I*bb*, and the boundary is a (001) twin boundary. The arrows in Figure 6 indicate the twin planes. Contrast analysis suggests this plane has II*b* (single "*b*") character and the interlayer including this plane has a II*b*+I*a* stacking sequence. Several twin boundaries have been investigated and all boundaries adopt this sequence (e.g., II*b* on the left of the brucite-like sheet and I*a* on the right, or visa versa). The frequency of twins is very high, which means that considerable amounts of II*b* sequence exist in the specimens (about 5%). However, no II*bb* interlayers were found.

Interstratified biotite/chlorite in altered granite. Biotite/chlorite interstratifications have been observed using HRTEM to investigate the chloritization mechanism (e.g., Veblen and Ferry 1983; Olives-banos and Amouric 1984; Eggleton and Banfield 1985). It is often proposed that interlayers of biotite, which contain potassium ions, can be changed to brucite-like interlayers, whereas T-O-T layers are inherited. Although the polytype of chlorite in the interstratification provides important information about the formation mechanism, chlorite polytypes have not been reported, probably due to the lack of a method to identify polytypes of thin (a few unit cells thick) packets of chlorite. An HRTEM image of a biotite/chlorite interstratification (Fig. 7) shows two brucite-like interlayers with I-type slant (indicated by the arrowheads); others have II-type slant. Polytype analysis reveals a mixture of I*bb*, I*ab*, II*ab*, and II*bb*, although II*bb* is dominant (Fig. 7). Different crystallization routes (e.g., precipitation from solution vs. solid state transformation) probably produce materials characterized by different degrees of polytypic disorder. Polytypes of products of direct transformations should be predictable, or partly constrained, based on reactant structures. Thus, polytypic details carry information about mineral paragenesis. Results for the biotite-to-chlorite transformation will be reported in detail separately (Kogure, Banfield, and Murakami, in preparation).

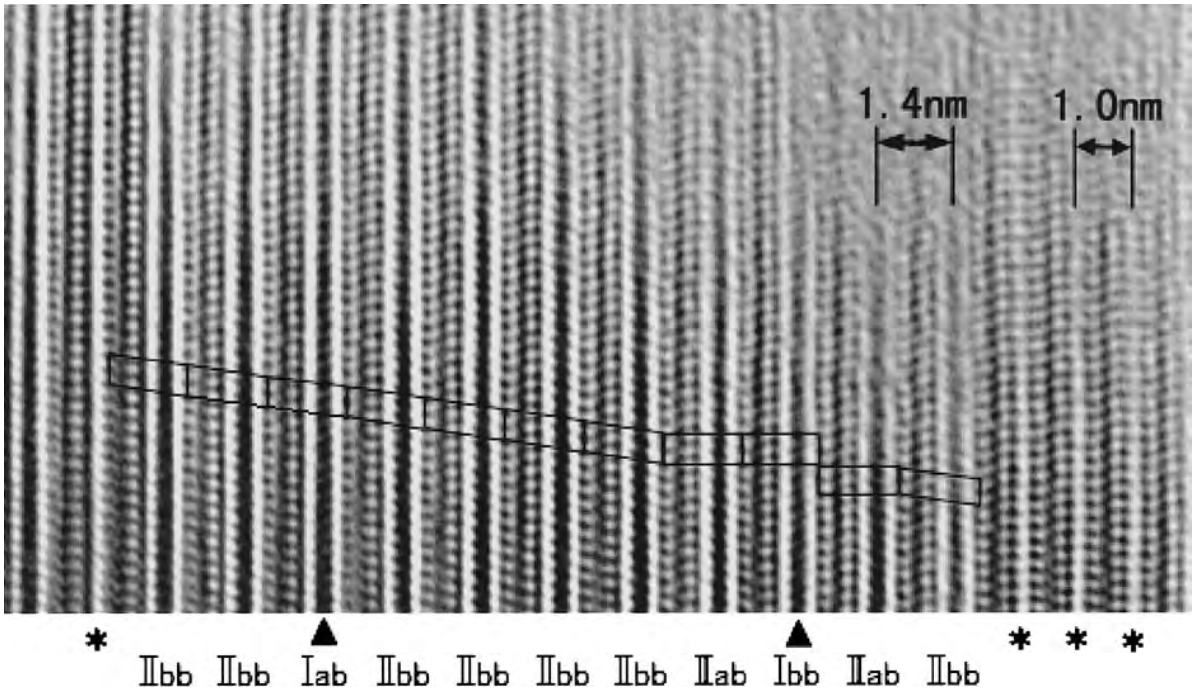

FIGURE 7. Filtered image of the interstratified biotite/chlorite in altered granite. Asterisks show biotite interlayers and arrowheads indicate I-type interlayers in chlorite. The parallelograms are a unit cell of each chlorite layer.

ACKNOWLEDGMENTS

We thank H. Shirozu and T. Murakami for donating several chlorite specimens. J.F.B. thanks S.W. Bailey for his suggestion that a method such as this might work. R. Reynolds and an anonymous reviewer are thanked for comments on the manuscript. J.F.B. acknowledges support from NSF grant no. EAR-9706382. The electron microscopy was performed in the Electron Microbeam Analysis Facility of the Mineralogical Institute, University of Tokyo.

REFERENCES CITED

Bailey, S.W. (1988a) X-ray diffraction identification of the polytypes of mica, serpentine, and chlorite. Clay and Clay Minerals, 36, 193–213.

———(1988b) Chlorites: structure and crystal chemistry. In Mineralogical Society of America Reviews in Mineralogy, 19, 347–403.

Banfield, J.F. and Bailey, S.W. (1996) Formation of regularly interstratified serpentine-chlorite minerals by tetrahedral inversion in long-period serpentine polytypes. American Mineralogist, 81, 79–91.

Banfield, J.F. and Murakami, T. (1998) Atomic-resolution transmission electron microscope evidence for the mechanism by which chlorite weathers to 1:1 semi-regular chlorite-vermiculite. American Mineralogist, 83, 348–357.

Bons, A.J. and Schryvers, D. (1989) High-resolution electron microscopy of stacking irregularities in chlorites from the central Pyrenees. American Mineralogist, 74, 1113–1123.

Brown, B.E. and Bailey, S.W. (1962) Chlorite polytypism: I. Regular and semirandom one-layer structures. American Mineralogist, 47, 819–850.

Eggleton, R.A. and Banfield, J.F. (1985) The alteration of granitic biotite to chlorite. American Mineralogist, 70, 902–910.

Jullien, M., Baronnet, A., and Goffé, B (1996) Ordering of the stacking sequence in cookeite with increasing pressure: An HRTEM study. American Mineralogist, 81, 67–78.

Kilaas, R. (1991) HREM image simulation. In G.W. Bailey, Ed., Proceeding of 49th EMSA meeting, p. 528–529. San Francisco Press, California.

———(1998) Optical and near-optical filters in high-resolution electron microscopy. Journal of Microscopy, 190, 45–51.

Kogure, T (1996) Investigation of alteration processes of biotite by high resolution electron microscopy. Ph.D. thesis. University of Tokyo, Japan.

Kogure, T. and Murakami, T. (1998) Structure and formation mechanism of low-angle grain boundaries in chlorite. American Mineralogist, 83, 358–364.

Olives-bamos, J. and Amouric, M. (1984) Biotite chloritization by interlayer brucitization as seen by HRTEM. American Mineralogist, 69, 869–871.

Shirozu, H. and Bailey, S.W. (1965) Chlorite polytypism: III. Crystal structure of an orthohexagonal iron chlorite. American Mineralogist, 50, 868–885.

Veblen, D.R. and Ferry, J.M. (1983) A TEM study of the biotite-chlorite reaction and comparison with petrologic observations. American Mineralogist, 68, 1160–1168.

Walker, J.R. (1993) Chlorite polytype geothermometry. Clays and Clay Minerals, 41, 260–267.

MANUSCRIPT RECEIVED FEBRUARY 3, 1998
MANUSCRIPT ACCEPTED MARCH 31, 1998
PAPER HANDLED BY ANNE M. HOFMEISTER